JACS
JOURNAL OF THE AMERICAN CHEMICAL SOCIETY

ARTICLE

pubs.acs.org/JACS

Regioselective Bis-functionalization of Endohedral Dimetallofullerene, $La_2@C_{80}$: Extremal La−La Distance

Midori O. Ishitsuka,[†] Shogo Sano,[†] Haruka Enoki,[†] Satoru Sato,[†] Hidefumi Nikawa,[†] Takahiro Tsuchiya,[†] Zdenek Slanina,[†] Naomi Mizorogi,[†] Michael T. H. Liu,[‡] Takeshi Akasaka,[*,†] and Shigeru Nagase[*,§]

[†]TARA Center, University of Tsukuba, Tsukuba, Ibaraki 305-8577, Japan

[‡]University of Prince Edward Island, Charlottetown, Prince Edward Island, Canada C1A4P3

[§]Department of Theoretical and Computational Molecular Science, Institute for Molecular Science, Okazaki, Aichi 444-8585, Japan

Supporting Information

ABSTRACT: Bis-functionalization of endohedral metallofullerene $La_2@C_{80}$ by carbene addition is reported herein. Adducts were characterized using spectroscopic and single-crystal X-ray structure analyses. Crystallographic data for bisadduct $La_2@C_{80}(CClPh)Ad$ (**3**, Ad = adamantylidene) revealed that both carbene additions occur at the 6,6-bond junction on the C_{80} cage with ring cleavages and that La atoms are positioned collinearly with spiro carbons. It is noteworthy that the La−La distance in **3** is highly elongated by carbene bis-functionalization compared to the distance in pristine $La_2@C_{80}$ and reported functionalized derivatives. The metal positions were confirmed through density functional calculations.

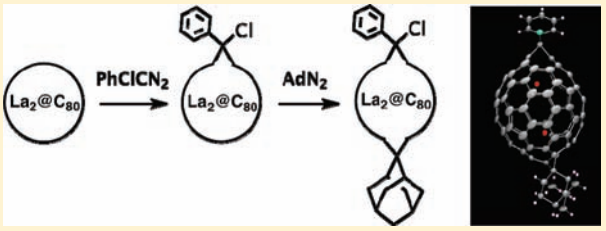

INTRODUCTION

Since the investigation of chemical functionalization of metallofullerenes is important for developing material science and other areas, many derivatization studies have been conducted.[1] Among these studies, a few bis-functionalizations of metallofullerene have been reported recently. Synthesis of $Gd_3N@C_{80}$ bis-adduct by 4+2 Diels−Alder-type cycloaddition was achieved, and mass spectra were used to confirm the assignment.[2] The bis-CF_3 derivative was synthesized through radical trifluoromethylation of $Sc_3N@C_{80}$; its structure was deduced using spectrometry and DFT calculation.[3] After synthesizing the bisadduct, $Sc_3N@C_{78}[C(COOEt)_2]_2$, using the Bingel−Hirsch reaction of $Sc_3N@C_{78}$,[4] Dorn et al. also reported synthesis of dibenzyl adducts of $M_3N@C_{80}$ (M = Sc, Lu), $M_3N@C_{80}(CH_2Ph)_2$, using a photochemical reaction.[5] In both cases, bisadducts were synthesized with high regioselectivity. The geometry of the second addition is supposed to be controlled by the internal trimetallic nitride cluster. Recently we reported the carbene bisadduct of non-IPR (isolated pentagon rule) dimetallofullerene, $La_2@C_{72}Ad_2$ (Ad = adamantylidene), which was obtained through stepwise photochemical carbene addition.[6] In this case, the reaction site of second addition might have been controlled by the first.

Meanwhile, because $La_2@C_{80}$ with an I_h symmetric carbon cage is a typical dimetallofullerene, many experimental and theoretical studies concerning $La_2@C_{80}$ have been undertaken to date. According to these studies, two encapsulated lanthanum atoms of this fullerene are known to rotate three-dimensionally inside the C_{80} fullerene sphere.[7] Furthermore, each metal atom donates three valence electrons to the carbon cage to form the electronic structure as $(La^{3+})_2C_{80}^{6-}$.[7a,8]

We synthesized silylated derivatives of $La_2@C_{80}$, $La_2@C_{80}(Ar_2Si)_2CH_2$ (Ar = Mes and Dep, Dep = 2,6-diethylphenyl), which revealed that two La atoms inside the cage of silylated endohedral metallofullerene hop two-dimensionally along the equator of the 1,4-silylated cage.[9] The 1,3-dipolar cycloaddition of $La_2@C_{80}$ afforded [6,6] and [5,6] adducts of endohedral pyrrolidinodimetallofullerene, $La_2@C_{80}(CH_2)_2NTrt$.[10] In the [6,6] adduct of this, the two metal atoms are fixed at slantwise positions on the mirror plane, whereas the metal atoms are collinear with the pyrrolidine ring in the [5,6] adduct. Selective addition of Ad to $La_2@C_{80}$ occurs at the [6,6]-bond junction with bond cleavage to afford the [6,6]-open-cage adduct, $La_2@C_{80}Ad$ (**1**).[11] Crystallographic analysis of **1** reveals that the two La atoms are collinear with the spiro carbon of the Ad moiety. It is interesting that the motion of metal atoms inside the cage is controllable by chemical modification from outside the fullerene cage. Moreover, a second functionalization of $La_2@C_{80}$ monoadduct is possible, and it warrants further investigation where the second addition occurs. In this context, we conducted bisfunctionalization of dimetallofullerene $La_2@C_{80}$ using the photochemical carbene addition. Herein, we report the syntheses and structural characterizations of the carbene monoadduct, $La_2@C_{80}(CClPh)$ (**2**), and the bisadduct, $La_2@C_{80}(CClPh)Ad$ (**3**).

Received: January 29, 2011
Published: April 15, 2011

EXPERIMENTAL SECTION

General. Toluene was distilled over benzophenone sodium ketyl under argon atmosphere prior to use for the reactions. *o*-Dichlorobenzene was distilled over P_2O_5 under vacuum before use. CS_2 was distilled over P_2O_5 under argon atmosphere before use. Reaction was monitored by HPLC with the following conditions: column, Buckyprep, diameter (ϕ) 4.6 mm × 250 mm; eluent, toluene; flow rate, 1.0 mL/min; temperature, 40 °C; detector, UV 330 nm. HPLC isolation was performed on an LC-908 or LC-918 instrument (Japan Analytical Industry Co. Ltd.). Mass spectrometry was performed (Biflex III, Bruker AXS GmbH) in negative and positive modes with 1,1,4,4-tetraphenylbutadiene as matrix. UV−vis spectra were measured in CS_2 solution using a spectrophotometer (UV-3150, Shimadzu Corp.). NMR spectra were obtained (Avance 500 and 300, Bruker AXS GmbH) in CS_2/$C_2D_2Cl_4$ (3/1) solution. The ^{13}C NMR shift was calibrated with 1,1,2,2-tetrachloroethane as an internal reference (δ = 73.8 ppm). Cyclic voltammograms (CVs) and differential pulse voltammograms (DPVs) were recorded using a electrochemical analyzer (CV50W, BAS Inc.). Platinum wires were used as the working and counter electrodes. The reference electrode was a saturated calomel reference electrode (SCE) filled with 0.1 M $(n\text{-Bu})_4NPF_6$ in 1,2-dichlorobenzene. CV: scan rate, 20 mV/s. DPV: pulse amplitude, 50 mV; pulse width, 50 ms; pulse period, 200 ms; scan rate, 20 mV/s.

Preparation and Purification of $La_2@C_{80}$. Soot containing lanthanide metallofullerenes was prepared according to the reported procedure using a composite anode containing graphite and the metal oxide with the atomic ratio of M/C equal to 2.0%.[15] The composite rod was subjected to an arc discharge as an anode under 150 Torr He pressure. Raw soot containing lanthanide metallofullerenes was collected and extracted with a 1,2,4-trichlorobenzene (TCB) solvent for 1.5 h. The soluble fraction was injected into the HPLC with a 5PYE column (ϕ 20 mm × 250 mm, Cosmosil, Nacalai Tesque Inc.) in the first step and a Buckyprep column (ϕ 20 mm × 250 mm, Cosmosil, Nacalai Tesque Inc.) in the second step to give pure $La_2@C_{80}$.

Photochemical Reaction of $La_2@C_{80}$ with Phenylchlorodiazirine. $PhClCN_2$ was synthesized and purified as reported in the literature.[16] A 27 mL toluene solution of $La_2@C_{80}$ (1.2 mg, 9.7×10^{-7} mol) and $PhClCN_2$ (4.4 mg, 2.9×10^{-5} mol) was placed in a Pyrex tube, degassed using freeze−pump−thaw cycles under reduced pressures, and then irradiated using a high-pressure mercury-arc lamp (50% cutoff <350 nm) at room temperature for 8 min. The adduct was isolated from unreacted $PhClCN_2$ and $La_2@C_{80}$ by preparative HPLC using a Buckyprep column (ϕ 20 mm × 250 mm; eluent, toluene) in the first step, with subsequent purification by recycling HPLC using a Buckyprep M column (ϕ 20 mm × 250 mm; eluent, toluene, 7 times recycling) in the second step to afford the pure adduct **2**.

$La_2@C_{80}$(CClPh) (**2**): ^1H NMR (500 MHz, $CS_2/C_2D_2Cl_4$ = 3/1) δ 8.95 (brs, 2H), 7.89−7.92 (m, 2H), 7.80 (t, J = 7.5 Hz, 1H); ^{13}C NMR (125 MHz, CS_2/CD_2Cl_4 = 3/1) δ 153.12 (1C), 153.10 (1C), 150.87 (1C), 150.77 (1C), 150.21 (1C), 150.01 (1C), 149.85 (1C), 149.79 (1C), 149.75 (1C), 149.71 (1C), 149.34 (1C), 149.28 (1C), 148.84 (1C), 148.81 (1C), 147.41 (1C), 147.32 (1C), 146.71 (1C), 146.64 (1C), 145.74 (1C), 145.71 (1C), 145.27 (1C), 145.10 (1C), 144.78 (1C), 144.45 (1C), 143.60 (1C), 143.57 (1C), 143.54 (1C), 143.32 (1C), 143.14 (1C), 142.95 (1C), 142.91 (1C), 142.49 (1C), 142.42 (1C), 142.34 (1C), 142.33 (1C), 140.65 (1C), 140.23 (1C), 140.12 (1C), 139.92 (1C), 139.66 (1C), 139.47 (1C), 137.00 (1C), 136.99 (1C), 136.90 (4C), 136.85 (1C), 136.76 (1C), 136.57 (1C), 136.55 (2C), 136.50 (1C), 136.39 (1C), 134.61 (1C), 134.58 (1C), 134.14 (1C), 134.09 (2C), 134.06 (1C), 134.04 (1C), 133.79 (1C), 133.69 (1C), 133.66 (1C), 133.61 (1C), 133.59 (1C), 133.50 (1C), 132.42 (1C), 131.18 (2C), 131.10 (1C), 130.11 (1C), 130.05 (d, 1C), 129.90 (1C), 129.57 (1C), 129.15 (d, 2C), 128.64 (d, 2C), 128.07 (1C), 124.87 (1C), 124.49 (1C), 122.87 (1C), 121.62 (1C), 117.86 (1C), 99.06 (1C), 64.59 (1C); MALDI-TOF mass m/z 1362 (M^-), 1327 ($M - Cl^-$); redox potentials (vs Fc/Fc^+) $^{ox}E_1$ = +0.52 V, $^{ox}E_2$ = +0.93 V, $^{red}E_1$ = −0.26 V, $^{red}E_2$ = −1.47 V, $^{red}E_3$ = −1.67 V.

Black crystals of **2**·$C_6H_4Cl_2$ were obtained by slow diffusion of hexane into a solution of **2** in *o*-dichlorobenzene. All measurements of the single-crystal X-ray analysis were performed at beamline BL-1A of the Photon Factory (KEK, Japan). Crystal data of $La_2@C_{80}$(CClPh)·$C_6H_4Cl_2$: $C_{93}H_9Cl_3La_2$, M_w = 1510.17, monoclinic, $P21/c$, a = 10.9639(5) Å, b = 20.6081(10) Å, c = 21.6433(13) Å, β = 101.468(3)°, V = 4792.6(4) Å^3, Z = 4, D_{calc} = 2.093 Mg/m^3, μ = 0.956 mm^{-1}, T = 100 K, crystal size 0.12 × 0.08 × 0.04 mm^3; 59 295 reflections (24 285 unique), 15 268 with $I > 2\sigma(I)$; R(int) = 0.0363, $R1$ = 0.1299 [$I > 2\sigma(I)$], w$R2$ = 0.3825 (all data); GOF (on F^2) = 1.021; maximum residual electron density =8.711 e Å^{-3}.

Photochemical Reaction of $La_2@C_{80}$(CClPh) (2) with Adamantane Diazirine. A 23 mL toluene solution of **2** (1.0 mg, 7.3×10^{-7} mol) and AdN_2 (6.0 mg, 3.7×10^{-5} mol) was placed in a Pyrex tube, degassed using freeze−pump−thaw cycles under reduced pressures, and then irradiated using a high-pressure mercury-arc lamp (50% cutoff <350 nm) at room temperature for 140 s. The reaction mixture was subjected to recycling HPLC using a Buckyprep column (ϕ 20 mm × 250 mm; eluent, toluene) to separate **3c** (adduct C) as well as a front fraction of mixed two adducts (A and B). Further purification of the fraction by recycling HPLC using a Buckyclutcher column (ϕ 20 mm × 250 mm; eluent, toluene; Sigma-Aldrich Inc.) gave the adducts A (**3a**) and B (**3b**).

$La_2@C_{80}$(CClPh)Ad, Adduct C (**3c**): ^1H NMR (300 MHz, CS_2/$C_2D_2Cl_4$ = 3/1) δ 8.92 (brs, 2H), 7.87 (t, J = 7.5 Hz, 2H), 7.80 (t, J = 7.5 Hz, 1H); UV−vis−NIR (CS_2) λ_{max} 484 nm; MALDI-TOF mass m/z 1496 (M^-), 1461 ($M - Cl^-$); redox potentials (vs Fc/Fc^+) $^{ox}E_1$ = +0.48 V, $^{ox}E_2$ = +0.91 V, $^{red}E_1$ = −0.41 V, $^{red}E_2$ = −1.54 V, $^{red}E_3$ = −1.89 V, $^{red}E_4$ = −2.28 V.

Black crystals of **3c**·$C_6H_5CH_3$ were obtained by slow diffusion of chloroform into a solution of **3c** in toluene. X-ray diffraction data were collected using an R-AXIS RAPID equipped with an imaging plate area detector using Mo Kα radiation. Crystal data of $La_2@C_{80}$(CClPh)Ad·$C_6H_5CH_3$: $C_{104}H_{27}ClLa_2$, M_w = 1589.53, monoclinic, $P21/c$, a = 10.948(2) Å, b = 23.752(4) Å, c = 21.215(4) Å, β = 96.123(7)°, V = 5485.3(18) Å^3, Z = 4, D_{calc} = 1.925 Mg/m^3, μ = 1.655 mm^{-1}, T = 120 K, crystal size 0.20 × 0.15 × 0.15 mm^3; 50 228 reflections (12 529 unique), 8437 with $I > 2\sigma(I)$; R(int) = 0.0803, $R1$ = 0.0571 [$I > 2\sigma(I)$], w$R2$ = 0.1324 (all data); GOF (on F^2) = 1.030; maximum residual electron density = 1.363 e Å^{-3}.

$La_2@C_{80}$(CClPh)Ad, Adduct A (**3a**): UV−vis−NIR (CS_2) λ_{max} 430, 483 nm; MALDI-TOF mass m/z 1496 (M^-), 1461 ($M - Cl^-$); redox potentials (vs Fc/Fc^+) $^{ox}E_1$ = +0.46 V, $^{ox}E_2$ = +1.11 V, $^{red}E_1$ = −0.48 V, $^{red}E_2$ = −1.66 V, $^{red}E_3$ = −1.87 V, $^{red}E_4$ = −2.28 V.

$La_2@C_{80}$(CClPh)Ad, Adduct B (**3b**): ^1H NMR (300 MHz, CS_2/$C_2D_2Cl_4$ = 3/1) δ 8.94 (brs, 2H), 7.89 (t, J = 7.5 Hz, 2H), 7.78 (t, J = 7.5 Hz, 1H); UV−vis−NIR (CS_2) λ_{max} 485 nm; MALDI-TOF mass m/z 1496 (M^-), 1461 ($M - Cl^-$); redox potentials (vs Fc/Fc^+) $^{ox}E_1$ = +0.45 V, $^{red}E_1$ = −0.41 V, $^{red}E_2$ = −1.63 V, $^{red}E_3$ = −1.81 V.

Theoretical Calculations. Geometries were optimized with the hybrid density functional theory at the B3LYP[17] level using the Gaussian 03 program.[18] The effective core potential and the corresponding basis set were used for La, and electrons in the outermost core orbitals were treated explicitly as valence electrons.[19] The contraction schemes used for the basis set were (5s5p3d)/[4s4p3d] for La in standard notation. The split-valence d-polarized 6-31G*[20] basis set was used for C, H, and Cl. For the calculations of ^{13}C NMR chemical shifts, the B3LYP-GIAO[21] method and the larger 6-311G*[22] basis set were used for C, H, and Cl.

dx.doi.org/10.1021/ja200903q |*J. Am. Chem. Soc.* 2011, 133, 7128–7134

Scheme 1

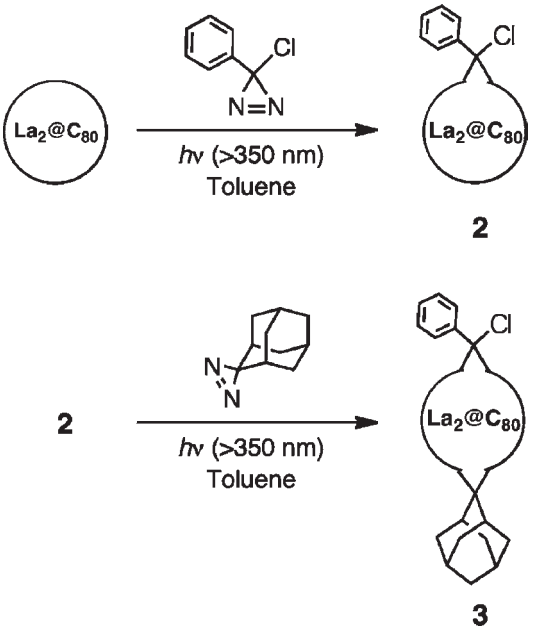

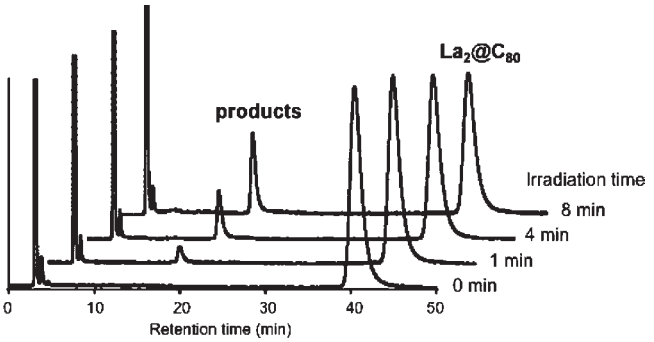

Figure 1. HPLC profiles of the reaction of $La_2@C_{80}$ with $PhClCN_2$. Conditions: Buckyprep column, ϕ 4.6 mm ×250 mm; eluent, toluene; UV monitored at 330 nm.

RESULTS AND DISCUSSION

Synthesis of $La_2@C_{80}$(CClPh). During our studies of derivatization of endohedral metallofullerenes by carbene addition, we conducted the photoreaction of $La_2@C_{80}$ with phenylchlorodiazirine ($PhClCN_2$), which is known to produce phenylchlorocarbene (:CClPh) exclusively by photolysis[12] (Scheme 1). A toluene solution of $La_2@C_{80}$ and an excess amount of $PhClCN_2$ was irradiated for several minutes (Figure 1). The resulting product was purified by preparative HPLC to enhance a major adduct predominantly, which was indicated as a carbene monoadduct, $La_2@C_{80}$(CClPh) (**2**), using matrix-assisted laser desorption/ionization time-of-flight (MALDI-TOF) mass spectrometry (Supporting Information). Considering the addition site, there are four possible structures for **2**, which has [6,6]-closed, [6,6]-open, [5,6]-closed, and [5,6]-open forms (Figure 2). The ^{13}C NMR spectrum of **2** showed 80 signals of the carbon cage aside from four signals of the phenyl group in the region of the aromatic carbon (Supporting Information), which indicates that **2** has a [6,6]-open-cage structure with C_1 symmetry. We can

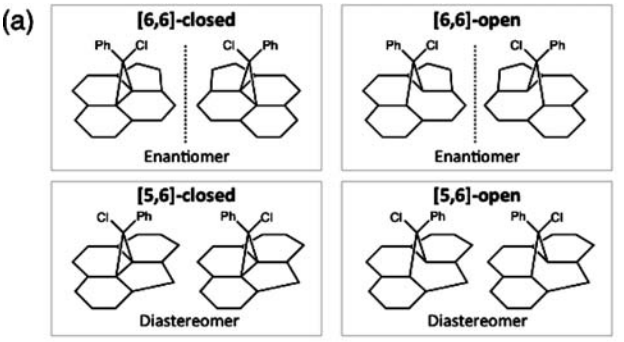

(b)

addition type	symmetry	signals of C_{80} cage		
		sp^2 carbon	sp^3 carbon	total
[6,6]-closed	C_1	1C×78	1C×2	80
[6,6]-open		1C×80	0	
[5,6]-closed	C_s	1C×8, 2C×35	2C×1	44
[5,6]-open		1C×8, 2C×36	0	

Figure 2. (a) Addition patterns of $La_2@C_{80}$(CClPh). (b) NMR patterns of $La_2@C_{80}$(CClPh) isomers.

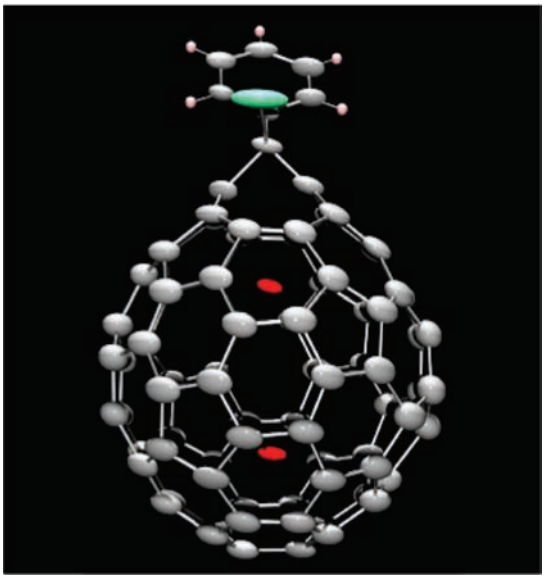

Figure 3. ORTEP drawing of **2** showing thermal ellipsoids at the 50% probability level. The *o*-dichlorobenzene molecule is omitted for clarity.

neglect [5,6] adducts because they should show 44 signals in ^{13}C NMR as a result of the C_s symmetry. A [6,6]-closed structure (C_1 symmetry) is also negligible because it has two sp^3 carbons of addition site on the C_{80} cage, but **2** shows no such sp^3 signals in ^{13}C NMR. Carbon signals of the carbene addition site in **2** appeared at 117.86 and 99.06 ppm. These values are similar to those found for related fullerene derivatives such as $La_2@C_{80}Ad$[11] and $Sc_3C_2@C_{80}Ad$.[13] Simulated values of ^{13}C NMR chemical shifts of **2** by theoretical calculation also support this structure (Supporting Information). Finally, the structure of **2** was determined using X-ray crystallographic analysis (Figure 3). Results showed that **2** is a [6,6]-open-cage adduct, and two La atoms inside the cage are located at collinear positions relative to the spiro carbon, as in the case of **1**.

dx.doi.org/10.1021/ja200903q |*J. Am. Chem. Soc.* 2011, 133, 7128–7134

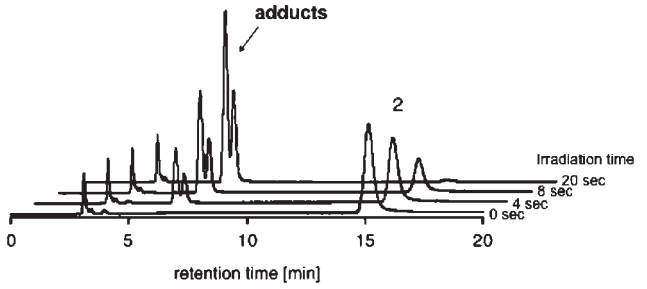

Figure 4. HPLC profiles of the reaction of **2** with AdN_2. Conditions: Buckyprep column, ϕ 4.6 mm × 250 mm; eluent, toluene; UV monitored at 330 nm.

The photochemical reaction of $La_2@C_{80}$ with $PhClCN_2$ affords $La_2@C_{80}(CClPh)$ (**2**) regioselectively in the same way as Ad addition. We conducted the second derivatization of **2** by carbene addition.

Synthesis of $La_2@C_{80}(CClPh)Ad$. We used Ad as a reactant in the second carbene addition because it has an advantage of high symmetry. A toluene solution of **2** and adamantane diazirine (AdN_2) was photoirradiated in the same way as the reaction with $PhClCN_2$ (Scheme 1). As shown in HPLC profiles of the reaction mixture, a peak of **2** disappeared after irradiation for 20 s, and new peaks corresponding to products appeared at earlier retention times as two peaks in the HPLC (Figure 4). **2** was entirely converted to products in this reaction. The products were purified using a multistep preparative HPLC to give three fractions; when several kinds of columns were used, each fraction was found to have a peak in HPLC. The amount ratios of the three fractions estimated from peaks in HPLC are almost the same. Each MALDI-TOF mass spectrum of three products showed a molecular ion peak (m/z 1496) corresponding to the molecular formula of $La_2@C_{80}(CClPh)Ad$ (**3**), in which the isotopic ratio of the measured molecular ion peak is consistent with the calculated one (Supporting Information). This result indicates that all of the reaction products are the bisadduct of $La_2@C_{80}$ connected with phenylchlorocarbene and Ad addends. It can be designated as a "hetero-bisadduct", which may be the first synthesized example of a bisadduct of endohedral metallofullerenes. We designated these three products as adducts A (**3a**), B (**3b**), and C (**3c**) in order of HPLC retention time using a Buckyclutcher column. It is notable that the second carbene addition affords only three isomeric adducts, although many possible addition sites exist in **2**. Furthermore, this reaction does not produce any multiadducts having more than two addenda. A second functionalization with carbene addition occurred regioselectively in this reaction.

Vis−NIR spectra of the three adducts (**3a**, **3b**, and **3c**) are portrayed in Figure 5, together with those of pristine $La_2@C_{80}$, $La_2@C_{80}Ad$ (**1**), and $La_2@C_{80}(CClPh)$ (**2**). The spectra of the three isomers are similar and resemble those of pristine $La_2@C_{80}$ and the monoadducts, **1** and **2**. These indicate that carbene addition to the fullerene cage does not affect the electronic features of these dimetallofullerenes.

Redox potentials of **2** and **3a**−**3c** were investigated using CV and DPV measurements. As Table 1 shows, the three isomers of the bisadduct have similar electronic character. They also resemble those of other derivatives and pristine $La_2@C_{80}$, which is in good agreement with the results of vis−NIR spectra of them. However, the first reduction potentials of **3a**−**3c** were

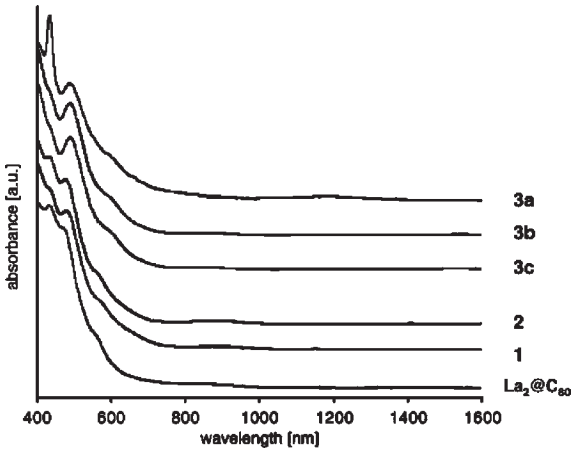

Figure 5. Vis−near-IR absorption spectra of $La_2@C_{80}$, **1**, **2**, and **3a**−**3c** in CS_2 solution.

Table 1. Redox Potentials[a] of $La_2@C_{80}$ and Its Derivatives

compound	$^{ox}E_2$	$^{ox}E_1$	$^{red}E_1$	$^{red}E_2$	$^{red}E_3$	$^{red}E_4$
3a	+1.11[b]	+0.46	−0.48	−1.66[b]	−1.87[b]	−2.28[b]
3b	–	+0.45	−0.41	−1.63[b]	−1.81[b]	–
3c	+0.91[b]	+0.48	−0.41	−1.54[b]	−1.89[b]	−2.28[b]
2	+0.93	+0.52	−0.26	−1.47[c]	−1.67[c]	–
1[e]	+0.86[b]	+0.49	−0.36	−1.78	−2.33[b]	–
$La_2@C_{80}$[d]	+0.95	+0.56	−0.31	−1.71	−2.13	–

[a] Versus Fc/Fc^+. In 1,2-dichlorobenzene with 0.1 M $(n\text{-}Bu)_4NPF_6$ at a Pt working electrode. CV, 20 $mV \cdot s^{-1}$. [b] Values are obtained by DPV. [c] Irreversible. [d] Data from ref 23. [e] Data from ref 11.

cathodically shifted slightly compared to that of **2**, similar to the cathodic shift of the first reduction potential of **1** compared to that of pristine $La_2@C_{80}$. Moreover, similar cathodic shifts are seen in the first oxidation potentials between **3a**−**3c** and **2** as well as **1** and pristine $La_2@C_{80}$, although the shift values are very small. These may indicate that the introduction of an Ad group results in a slight decrease of the electron-accepting properties of $La_2@C_{80}$.

Unfortunately, we have not been able to measure ^{13}C NMR of bisadducts because of poor solubility in appropriate NMR solvent. Furthermore, the fact that the structures of bisadducts derived from **2** are all in a C_1 symmetry engenders difficulty with the structural determination using spectroscopy. Therefore, we have theoretically predicted the addition site of carbene addend on the fullerene cage. Charge densities and π-orbital axial vector analysis (POAV) angles[14] of all carbon atoms on the cage of **2** were calculated (Supporting Information). The results show that the carbons that have high negative charges are located mainly at the opposite side of the cage from a CClPh substitute. Among these, four carbons (C1, C2, C3, and C4) have much larger negative charges and larger POAV angles compared to those of other carbons (Figure 6). Because the electron-deficient Ad may act as an electrophile in this reaction, Ad: is presumed to attack more electronegative carbons of the cage. The calculated result that the POAV angle of C1 is the largest value among all of carbons indicates that Ad: may attack the bonds of C1−C2, C1−C3, or C1−C4 to afford isomers A, B, and C, respectively. This can explain the formation of three isomers in this reaction.

dx.doi.org/10.1021/ja200903q | J. Am. Chem. Soc. 2011, 133, 7128–7134

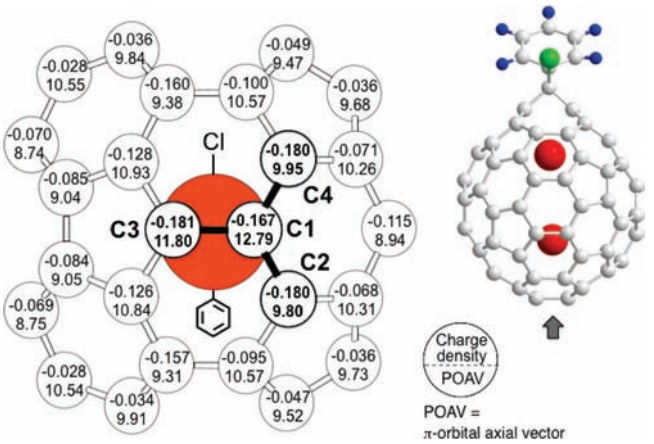

Figure 6. Selected Mulliken atomic charges (upper) and POAV values (lower) in **2**.

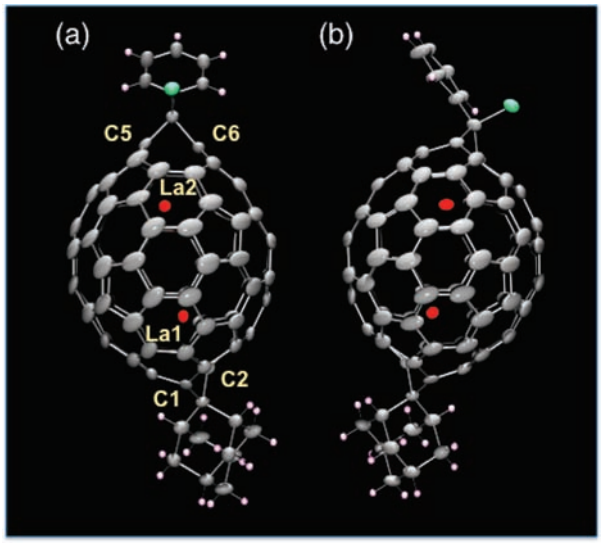

Figure 7. Front and side view ORTEP drawings of **3c** showing thermal ellipsoids at the 50% probability level. The toluene molecule is omitted for clarity.

The relative energies for the isomers A, B, and C are 0.291, 0, and 0.282 kcal/mol, respectively, obtained by DFT calculations at the B3LYP level.

We conducted a single-crystal X-ray crystallographic analysis for one of the three adducts, $La_2@C_{80}$(CClPh)Ad adduct C (**3c**). The molecular structure of **3c** was revealed unambiguously as shown in Figure 7. Results show that Ad: adds to the bond C1−C2 to afford isomer A, which is the site predicted above. The second carbene addition was controlled regioselectively to afford the bisadduct. The distance between C1 and C2 (2.14 Å) in the crystal structure of **3c** shows that the C1−C2 bond between two six-membered rings was broken by carbene addition to afford the open-cage structure. Two La atoms in **3c** are located underneath each addition site and are collinear with a spiro carbon of carbene addendum. Distances of La1−C1 (2.63 Å), La1−C2 (2.62 Å), La2−C5 (2.63 Å), and La2−C6 (2.56 Å) are all close to 2.6 Å, similar to those of **1** and **2**. However, it is notable that the distance of La1−La2 in **3c** is 4.16 Å, which is clearly longer than those of the monoadducts.

Table 2. La−La Distances (Å) in $La_2@C_{80}$ and Its Derivatives As Determined Using Single-Crystal X-ray Crystallographic Analyses and Theoretical Calculations

compound	crystallographic analysis	calculation[a]
$La_2@C_{80}$	3.84[b]	3.74[c]
$La_2@C_{80}(Dep_2Si)_2CH_2$	3.793(1)[d]	–
$La_2@C_{80}(CH_2)_2NTrt$	3.823(1)[e]	3.71[e]
$La_2@C_{80}$Ad (**1**)	4.031(1)[f]	3.89[f]
$La_2@C_{80}$(CPhCl) (**2**)	4.013(1)	3.91
$La_2@C_{80}$(CPhCl)Ad (**3a**)	4.159(3)	4.09

[a] All calculation were carried out at the HF and B3LYP level. [b] Data from ref 7c. [c] Data from ref 24. [d] Data from ref 9. [e] Data from ref 10. [f] Data from ref 11.

The La−La distances in $La_2@C_{80}$ and its derivatives are presented in Table 2; the values are derived from the X-ray crystallographic structure and theoretically optimized structure. Schematics of all structures are depicted in Figure 8. The experimental values according to the substituted group appears to be in agreement with the calculated ones. The La−La distance of pristine $La_2@C_{80}$ is 3.84 Å, as derived from the structure analyzed using synchrotron radiation power diffraction using the MEM/Rietvelt method.[7c] The values in $La_2@C_{80}(Ar_2Si)_2CH_2$ (3.80 Å)[9] and [6,6]-$La_2@C_{80}(CH_2)_2$NTrt (3.82 Å)[10] are almost identical to those of pristine $La_2@C_{80}$. However, the La−La distances in **1** (4.03 Å)[11] and **2** (4.01 Å) are 0.2 Å longer than that in pristine $La_2@C_{80}$. The La−La elongation in **1** and **2** can be attributed to the expansion of the inner space of the cage caused by a bond cleavage, which reduces the electrostatic repulsion between positively charged La atoms. For $La_2@C_{80}(Ar_2Si)_2CH_2$ and [6,6]-$La_2@C_{80}(CH_2)_2$NTrt, chemical modification of $La_2@C_{80}$ leads the motion of two La atoms to two-dimensional circulation or being still at the slantwise position, respectively, but the La−La distance of these does not change, perhaps because the inner spaces of their cages do not change. However, in the case of carbene bis-adduct **3c**, which has two bond cleavages on the cage, the La−La distance (4.16 Å) is much more elongated. Hence, the distance between two La atoms can be changed by functionalization of the carbon cage.

Regarding the electronic structure, **2** and **3** are formally designated as $[La_2]^{6+}[C_{80}(CClPh)]^{6-}$ and $[La_2]^{6+}[C_{80}(CClPh)Ad]^{6-}$, respectively. We calculated the electrostatic potentials of the fullerene sphere of $[C_{80}(CClPh)]^{6-}$ and $[C_{80}(CClPh)Ad]^{6-}$. Their resultant electrostatic potential maps are presented in Figure 9, along with the reported ones of $[C_{80}]^{6-}$[8] and $[C_{80}Ad]^{6-}$.[11] Positively charged metal atoms are expected to be highly stabilized at the minimum of electrostatic potentials inside the carbon cage. In pristine $La_2@C_{80}$ there is no minimum in electrostatic potentials. Therefore, the La atoms are not immobile; instead, they are circulating randomly inside the cage. However, the potential map of $[C_{80}Ad]^{6-}$ shows a minimum near the bottom of the cage, and $[C_{80}(CClPh)]^{6-}$ shows a similar pattern in its map. In both cases, one of the two La atoms can be expected to be stabilized at the minimum point; another can be expected to be located far away from it because of their electronic repulsion. These La positions are coincident with those shown in their X-ray crystallographic structures. Additionally, it is noteworthy that the two minimum points are visible in the potential maps of $[C_{80}(CClPh)Ad]^{6-}$, and that the

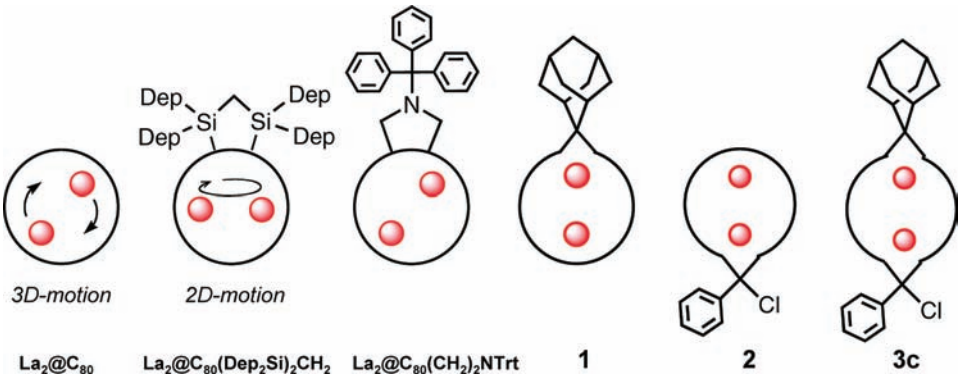

Figure 8. Metal atom positions in $La_2@C_{80}$, $La_2@C_{80}(Ar_2Si)_2CH_2$, [6,6]-$La_2@C_{80}(CH_2)_2NTrt$, **1**, **2**, and **3c**.

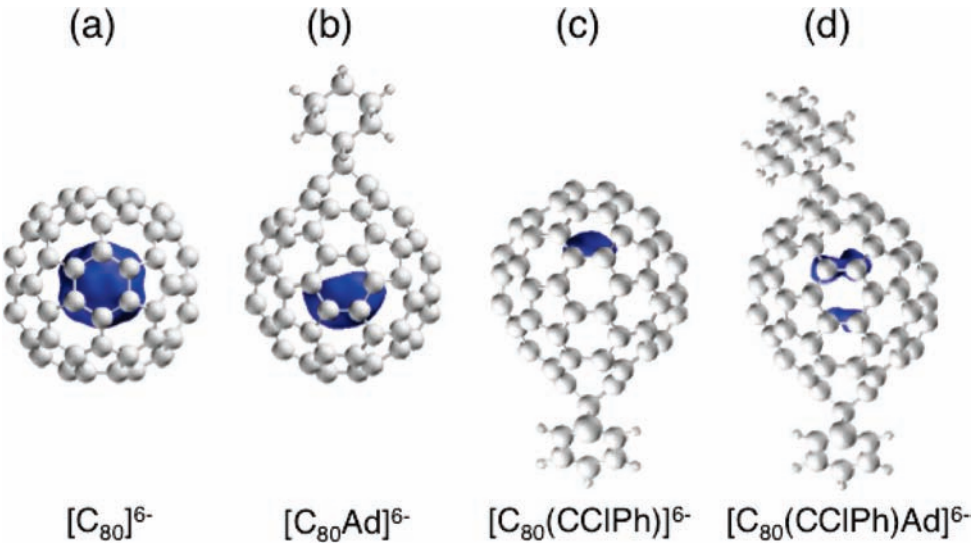

Figure 9. Electrostatic potential maps of (a) $[C_{80}]^{6-}$,[8] (b) $[C_{80}Ad]^{6-}$,[11] (c) $[C_{80}(CClPh)]^{6-}$, and (d) $[C_{80}(CClPh)Ad]^{6-}$.

distance between two minima is consistent with the La−La distance indicated by X-ray crystallographic analysis of **3c**. We presume that the clear appearance of two minima in the electrostatic potential map leads to the elongation of La−La distance in bisadduct.

CONCLUSIONS

We have described bis-functionalization of endohedral metallofullerene $La_2@C_{80}$ by carbene addition. Derivatization was conducted stepwise using different carbenes to afford "hetero-bisadduct", in which the addition occurred in a high yield and regioselective manner in each step. The monoadduct and bisadduct, **2** and **3**, were characterized using MALDI-TOF-mass, UV−vis, NMR spectroscopy, and a single-crystal X-ray crystallographic analysis. Both carbene additions took place at the 6,6-bond junction, along with bond cleavages on the C_{80} cage to afford the open-cage structure. It is noteworthy that the La−La distance in **3c** was clearly elongated compared to that in **1** and **2**, which is explained by the expansion of the inner space of the cage caused by the bond cleavage allowing two La atoms to separate, further reducing the electrostatic repulsion between positively charged atoms. In addition, the position of two La atoms in **2** and **3c** was confirmed through density functional calculations. The regioselectivity of the second carbene addition to **2** showed good agreement with the theoretical calculation, in which an electrodeficient carbene attacks the larger negative-charged and larger bond-strained carbon.

ASSOCIATED CONTENT

Supporting Information. Complete ref 18, crystallographic data in CIF format, spectroscopic data for **2** and **3c**, and calculated ^{13}C NMR chemical shifts, charge densities, and POAV values of **2**. This material is available free of charge via the Internet at http://pubs.acs.org.

AUTHOR INFORMATION

Corresponding Author
akasaka@tara.tsukuba.ac.jp

ACKNOWLEDGMENT

This work was supported in part by a Grant-in-Aid for Scientific Research on Innovative Areas (No. 20108001, "pi-Space"), a Grant-in-Aid for Scientific Research (A) (No. 20245006) and (C) (No. 21550032), The Next Generation Super Computing

Project (Nanoscience Project), Nanotechnology Support Project, Grants-in-Aid for Scientific Research on Priority Area (Nos. 20036008, 20038007), and Specially Promoted Research from the Ministry of Education, Culture, Sports, Science, and Technology of Japan, and The Strategic Japanese-Spanish Cooperative Program funded by JST and MICINN. S.S. thanks the Japan Society for the Promotion of Science (JSPS) for the Research Fellowship for Young Scientists.

REFERENCES

(1) (a) *Chemistry of Nanocarbons*; Akasaka, T., Wudl, F., Nagase, S., Eds.; John Wiley & Sons Ltd.: Chichester, 2010. (b) *Endofullerenes: A New Family of Carbon Clusters*; Akasaka, T., Nagase, S., Eds.; Kluwer Academic Publishers: Dordrecht, 2002.

(2) Stevenson, S.; Stephen, R. R.; Amos, T. A.; Cadorette, V. R.; Reid, J. E.; Phillips, J. P. *J. Am. Chem. Soc.* **2005**, *127*, 12776–12777.

(3) Shustova, N. B.; Popov, A. A.; Mackey, M. A.; Coumbe, C. E.; Phillips, J. P.; Stevenson, S.; Strauss, S. H.; Boltalina, O. V. *J. Am. Chem. Soc.* **2007**, *129*, 11676–11677.

(4) Cai, T.; Xu, L.; Shu, C.; Champion, H. A.; Reid, J. E.; Anklin, C.; Anderson, M. R.; Gibson, H. W.; Dorn, H. C. *J. Am. Chem. Soc.* **2008**, *130*, 2136–2137.

(5) Shu, C.; Slebodnick, C.; Xu, L.; Champion, H.; Fuhrer, T.; Cai, T.; Reid, J. E.; Fu, W.; Harich, K.; Dorn, H. C.; Gibson, H. W. *J. Am. Chem. Soc.* **2008**, *130*, 17755–17760.

(6) Lu, X.; Nikawa, H.; Tsuchiya, T.; Maeda, Y.; Ishitsuka, M. O.; Akasaka, T.; Toki, M.; Sawa, H.; Slanina, Z.; Mizorogi, N.; Nagase, S. *Angew. Chem. Int. Ed.* **2008**, *47*, 8642–8645.

(7) (a) Kobayashi, K.; Nagase, S.; Akasaka, T. *Chem. Phys. Lett.* **1996**, *261*, 502–506. (b) Akasaka, T.; Nagase, S.; Kobayashi, K.; Waelchli, M.; Yamamoto, K.; Funasaka, H.; Kako, M.; Hoshino, T.; Erata, T. *Angew. Chem., Int. Ed. Engl.* **1997**, *36*, 1643–1645. (c) Nishibori, E.; Takata, M.; Sakata, M.; Taninaka, A.; Shinohara, H. *Angew. Chem., Int. Ed.* **2001**, *40*, 2998–2999. (d) Shimotani, H.; Ito, T.; Iwasa, Y.; Taninaka, A.; Shinohara, H.; Nishibori, E.; Takata, M.; Sakata, M. *J. Am. Chem. Soc.* **2004**, *126*, 364–369.

(8) (a) Kobayashi, K.; Nagase, S.; Akasaka, T. *Chem. Phys. Lett.* **1995**, *245*, 230–236. (b) Kobayashi, K.; Nagase, S. *Chem. Phys. Lett.* **1996**, *262*, 227–232.

(9) Wakahara, T.; Yamada, M.; Takahashi, S.; Nakahodo, T.; Tsuchiya, T.; Maeda, Y.; Akasaka, T.; Kako, M.; Yoza, K.; Horn, E.; Mizorogi, N.; Nagase, S. *Chem. Commun.* **2007**, 2680–2682.

(10) (a) Yamada, M.; Wakahara, T.; Nakahodo, T.; Tsuchiya, T.; Maeda, Y.; Akasaka, T.; Yoza, K.; Horn, E.; Mizorogi, N.; Nagase, S. *J. Am. Chem. Soc.* **2006**, *128*, 1402–1403. (b) Yamada, M.; Okamura, M.; Sato, S.; Someya, C. I.; Mizorogi, N.; Tsuchiya, T.; Akasaka, T.; Kato, T.; Nagase, S. *Chem. Eur. J.* **2009**, *15*, 10533–10542.

(11) Yamada, M.; Someya, C.; Wakahara, T.; Tsuchiya, T.; Maeda, Y.; Akasaka, T.; Yoza, K.; Horn, E.; Liu, M. T. H.; Mizorogi, N.; Nagase, S. *J. Am. Chem. Soc.* **2008**, *130*, 1171–1176.

(12) Liu, M. T. H. *Chemistry of Diazirines*; CRC Press: Boca Raton, FL, 1987.

(13) Iiduka, Y.; Wakahara, T.; Nakahodo, T.; Tsuchiya, T.; Sakuraba, A.; Maeda, Y.; Akasaka, T.; Yoza, K.; Horn, E.; Kato, T.; Liu, M. T. H.; Mizorogi, N.; Kobayashi, K.; Nagase, S. *J. Am. Chem. Soc.* **2005**, *127*, 12500–12501.

(14) Haddon, R. C. *Science* **1993**, *261*, 1545–1550.

(15) Yamamoto, K.; Funasaka, T.; Takahashi, T.; Akasaka, T.; Suzuki, T.; Maruyama, Y. *J. Phys. Chem.* **1994**, *98*, 12831–12833.

(16) Graham, W. H. *J. Am. Chem. Soc.* **1965**, *87*, 4396–4397.

(17) (a) Becke, A. D. *Phys. Rev. A* **1988**, *38*, 3098–3100. (b) Becke, A. D. *J. Chem. Phys.* **1993**, *98*, 5648–5652. (c) Lee, C.; Yang, W.; Parr, R. G. *Phys. Rev. B* **1988**, *37*, 785–789.

(18) Frisch, M. J.; *GAUSSIAN 03*, revision C. 01; Gaussian Inc.: Wallingford, CT, 2004.

(19) Hay, P. J.; Wadt, W. R. *J. Chem. Phys.* **1985**, *82*, 299–310.

(20) Hehre, W. J.; Ditchfield, R.; Pople, J. A. *J. Chem. Phys.* **1972**, *56*, 2257–2261.

(21) Wolinski, K.; Hilton, J. F.; Pulay, P. *J. Am. Chem. Soc.* **1990**, *112*, 8251–8260.

(22) Krishnan, R.; Binkley, J. S.; Seeger, R.; Pople, J. A. *J. Chem. Phys.* **1980**, *72*, 650–654.

(23) Suzuki, T.; Maruyama, Y.; Kato, T.; Kikuchi, K.; Nakao, Y.; Achiba, Y.; Kobayashi, K.; Nagase, S. *Angew. Chem., Int. Ed. Engl.* **1995**, *34*, 1094–1096.

(24) Kubozono, Y.; Takabayashi, Y.; Kashino, S.; Kondo, M.; Wakahara, T.; Akasaka, T.; Kobayashi, K.; Nagase, S.; Emura, S.; Yamamoto, K. *Chem. Phys. Lett.* **2001**, *335*, 163–169.